Journal of the European Ceramic Society 19 (1999) 2027–2032

PII: S0955-2219(99)00014-X
0955-2219/99/$ - see front matter

Local Chemistry Changes in Si_3N_4 Based Ceramics During Hot-pressing and Subsequent Annealing

K. Rajan[a] and P. Šajgalík,[b]*

[a]Rensselaer Polytechnic Institute, Materials Science and Engineering Department, Troy, New York 12180-3590, USA
[b]Institute of Inorganic Chemistry, Slovak Academy of Sciences, Dúravská cesta 9, SK-842 36 Bratislava, Slovakia

(Received 20 May 1998; accepted 12 December 1998)

Abstract

The local chemistry changes within the triple points of the Si_3N_4 based ceramics are discussed. The extents of Fe, Cr and Ti impurities segregation and coalescence after crystallization of the triple point were determined. These impurities were present also prior to crystallization in the glassy triple pockets but they were distributed over the whole volume of the triple pockets and were thus under the detection limits of the EDX method. The paper indicates that these coalesced impurities are responsible for cavity formation in the Si_3N_4 based composites studied.

Keywords: hot pressing, electron microscopy, microstructure: final, impurities, Si_3N_4.

1 Introduction

Silicon nitride based ceramics have been intensively studied during recent decades. They have recently found application in the automotive industry. Ceramic parts are serially mounted into cars in Japan and exhaust valves are close to serial application in Germany. The main goal in ceramic research is to understand the processes occurring during material preparation and to relate these to the material performance. The reason for this is to design a chemically and thermodynamically stable ceramic material which is able to retain good mechanical properties under long-term high-temperature conditions.[1–4] These requirements for ceramic parts put strict requirements on the material, particularly for the chemical stability of the phases present. In spite of intensive study, questions concerning the micro-chemistry and thermodynamic stability are still open. The fact that ceramics based on silicon nitride are polycrystalline materials consisting of major crystalline β–Si_3N_4 phase and several minor oxide phases, which can be in the amorphous and/or crystalline status,[5–7] makes the understanding of their high-temperature behavior difficult. The residual oxide phases significantly affect high-temperature properties following their use as sintering additives. However, the role of impurities introduced along with the silicon nitride itself is also not negligible.[8]

The present paper attempts to point out the changes in the local chemistry of a Si_3N_4 composite prepared by hot-pressing with Al_2O_3 and Y_2O_3 as sintering additives and reinforced with β-Si_3N_4 whiskers.

2 Experimental

The β-Si_3N_4 whisker reinforced Si_3N_4 composites used for the present study were prepared by hot-pressing at a temperature of 1750°C and a pressure of 30 MPa in a static nitrogen atmosphere with overpressure 30 kPa. Eight wt% of Al_2O_3 (99·9%) and Y_2O_3 (99·99%) were added as the sintering additives in the molar ratio 3:5 to the Si_3N_4 crystalline powder (H1-H.C. Starck, > 95 wt% α phase, main impurities: oxygen 1·6 wt%, carbon 0·5 wt% and < 500 ppm other impurities). The experimental procedure for β-Si_3N_4 whisker dispersion in the Si_3N_4 matrix is described in detail in Refs 9 and 10. The whiskers had a mean aspect ratio of ~5 and were prepared by the SHS (self-propagating high-temperature synthesis) method; their characteristics are described in Ref. 11. The chemical analysis of the whisker composition is given in Table 1. The dilatometry of the composites during

*To whom correspondence should be addressed.

Table 1. Chemical characterization of the β-Si_3N_4 whiskers. Si, N, chemical analysis; O, C, neutron activation analysis; rest, spectral analysis (amounts are in wt%)

Si	*N*	*O*	*C*	*Ni*	*Al*	*Fe*	*B Ti, Cr, Mg*	*Cu, Ag,*	*Ca*
60·00	37·41	2·44	0·10	0·05–0·10	0·01–0·05	0·10–0·50	0·005–0·01	0·001–0·005	0·005–0·01

sintering was performed in a horizontal dilatometer ASTRO at 1850°C in nitrogen atmosphere.

Hot-pressed dense composite specimens containing 20 wt% of β-Si_3N_4 whiskers were embedded in BN powder and annealed to crystallise the triple points. The annealing regime was as follows: isothermal annealing for 24 h at 1400°C and then temperature decrease from 1400 to 1200°C for 25 h in a nitrogen atmosphere of 4 MPa. Crystalline phases were identified at the polished surface by X-ray diffraction, the local chemistry has been studied on thin foils by means of transmission electron microscopy (TEM). Thin foils were prepared by conventional ion-thinning techniques and these were coated by gold/carbon for TEM. The samples coated with gold were used specially for carbon content assessment. A CM-12 Philips TEM with EDX (energy disperse X-ray) analytical capabilities for light elements was used. A spot size of 30 nm was used for the elemental analysis. In-situ crystallisation of amorphous triple points was performed in TEM by using an intensive electron beam.

The cavity formation and evolution were studied on the tensile surface of testing bars which had been subjected to a creep test. The creep conditions were as follows: stress range 50–125 MPa at 1200°C in four-point bending (with 20/40 mm inner/outer spans) in air.

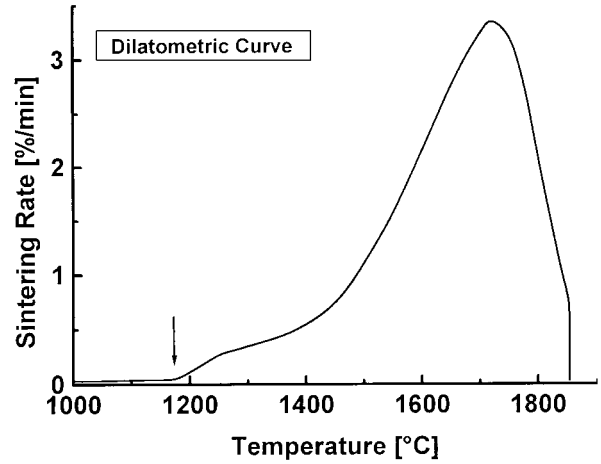

Fig. 1. Dilatometric curve of sintered β-Si_3N_4 whisker reinforced Si_3N_4 composite. The arrow shows the temperature at which the shrinkage of the sample starts.

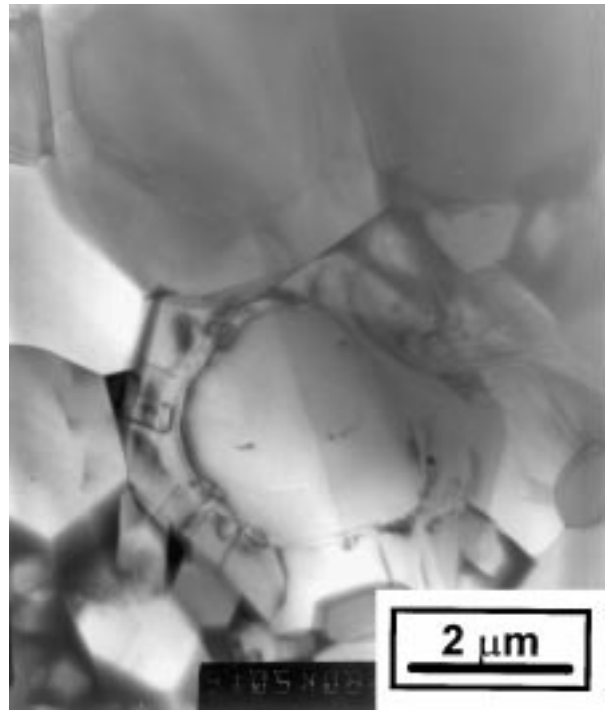

Fig. 2. TEM micrograph of Si_3N_4 ceramics prepared in present study.

3 Results and Discussion

The measurement of the dilatometric curves during sintering showed that the shrinkage always starts below/at 1200°C; an example is shown in Fig. 1 The lowest temperature of liquid phase formation in the quasi-binary $Al_5Y_3O_{12}$–SiO_2 system for a wide range of SiO_2 additions is approx. 1350°C.[12] The present starting composition of sintering additives chemically corresponds to this quasi-binary system, where the SiO_2 is introduced as a surface impurity of the raw Si_3N_4 powder. A possible explanation for the discrepancy between these temperatures is the presence of impurities introduced along with the whiskers (see Table 1) and starting powders.

The EDX analysis of glassy pockets formed from the liquid at the temperature of hot-pressing shows the presence of the main elements, i.e. Si, Y, Al and O. The other impurities listed in Table 1 are not detected by EDX. These are probably dissolved in the liquid phase at the temperature of hot-pressing, but their amount is under the detection limit of the EDX system.

A TEM micrograph characterizing the present composite is given in Fig. 2. The microstructure consists of β-Si_3N_4 grains and the grain boundary

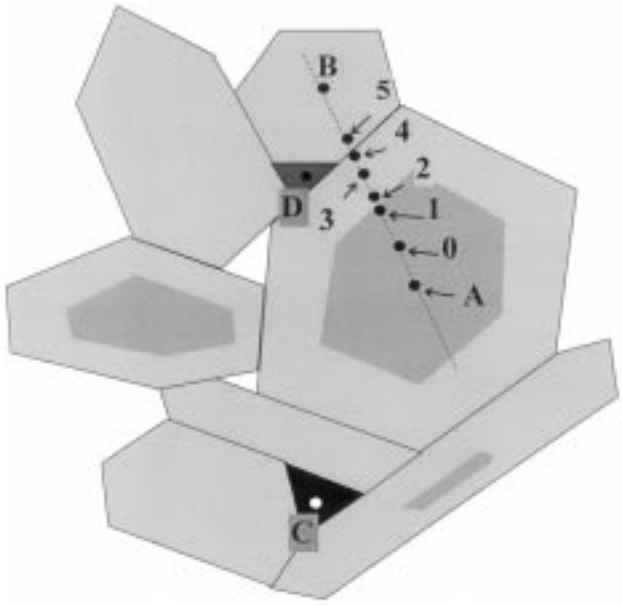

Fig. 3. Schematic of the microstructure, spots A, B, C, D, 0, 1, 2, 3, 4, 5 represent the points of EDX analyses.

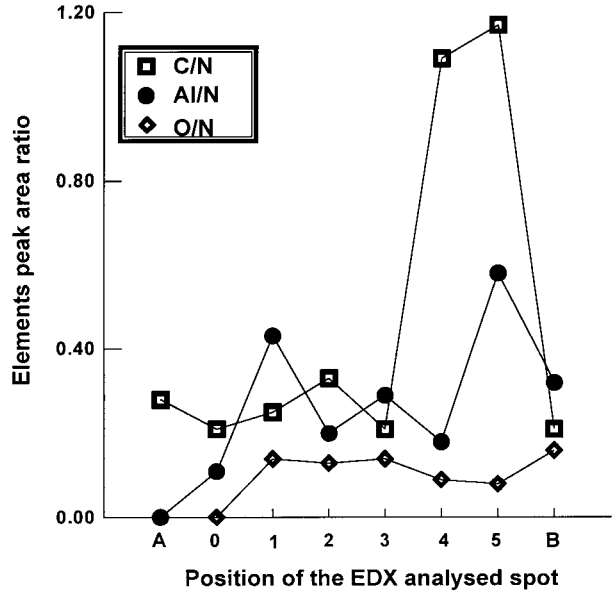

Fig. 4. EDX analyses from the spots shown in Fig. 2. The element concentration ratio is considered to be related to the element peak area ratio.

phases. The section of the β-Si_3N_4 grain in Fig. 2 reveals that the grain consists of a core and a shell. The shell is grown on the original β-Si_3N_4 grain pre-existing in the starting powder. These pre-existing β-Si_3N_4 grains are important for the heterogeneous nucleation of β-Si_3N_4 phase.[13]

The spatial location of the spots for EDX analysis is depicted in the schematic of the TEM micrograph shown in Fig. 3. The results of EDX analysis for the centers of grains and for triple points are summarized in Table 2.

The EDX spectra of the spot series localized on the line from A to B have been evaluated and the elemental analyses of the local chemistry are shown in Fig. 4. It is seen that the ratios of O/N and Al/N are step-wise changed at the sub-grain boundary of the grain (spot 1 in Fig. 4) grown from the β-Si_3N_4 heterogeneous nuclei during phase transformation and subsequent grain growth. While the Al/N shows also a second maximum at the grain boundary between two Si_3N_4 grains, the O/N ratio remains almost constant. The solubility of yttrium was below the detection limit.

These results are consistent with the results of Krämmer *et al.*[14] Fig. 4 also shows that the ratio of

Table 2. EDX analysis of the centers of grains and triple points, according to the schematic shown in Fig. 3[a]

Spot	*Si*	*Al*	*O*	*N*	*Y*
A	↑	—	—	↑	—
B	↑	↕	↓	↑	—
C	↑	↕	↕	↓	↕
C	↑	↕	↕	↓	↕
D	↑	↑	↑	↓	↑

[a]Legends: ↑ strong peak, ↕ weak peak, ↓ trace,—not present.

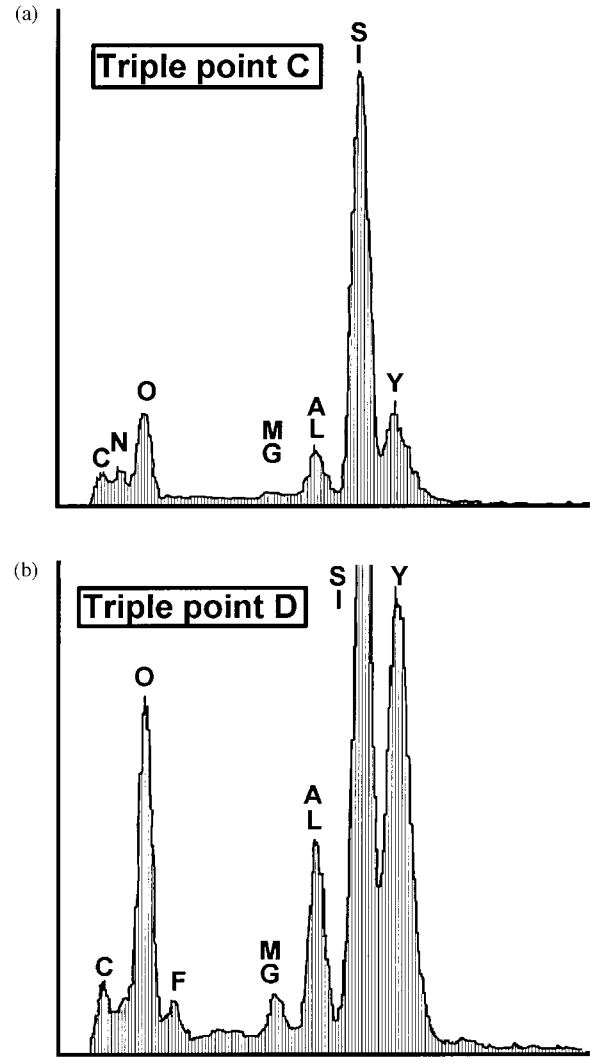

Fig. 5. (a) EDX analysis of triple point C (see Fig. 3). (b) EDX analysis of triple point D (see Fig. 3).

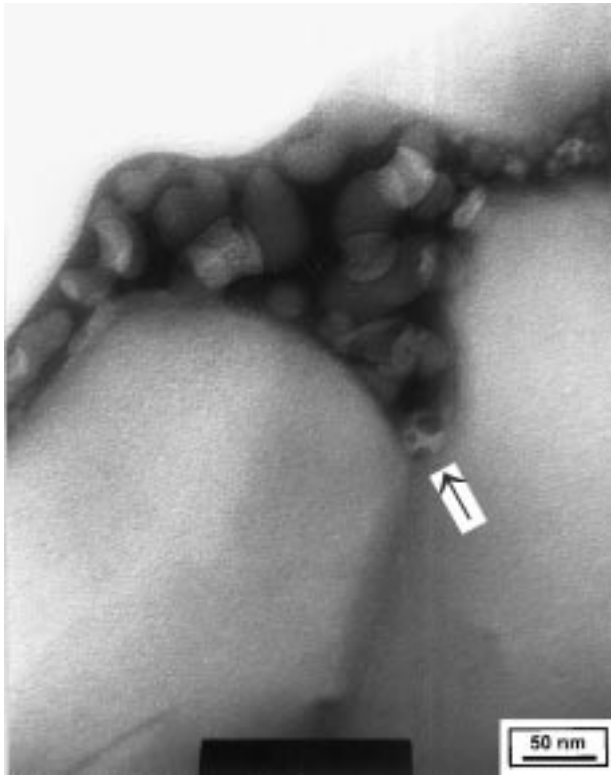

Fig. 6. TEM micrograph of in-situ crystallized amorphous region.

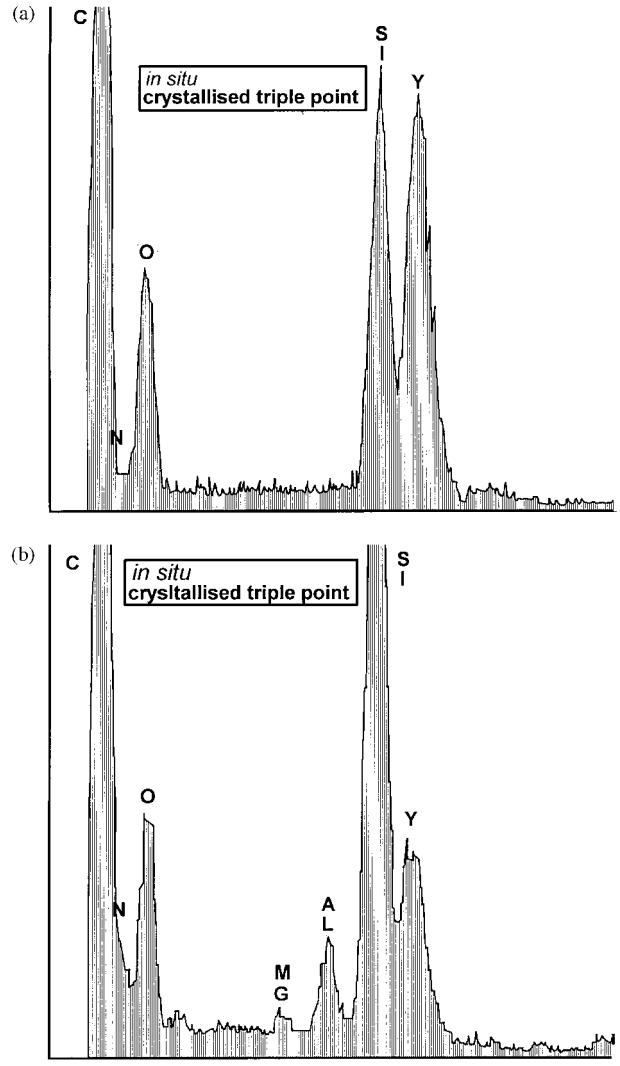

Fig. 7. (a) EDX analysis of the in-situ crystallized triple point. (b) EDX analysis of the in-situ crystallized triple point.

C/N is drastically changed at the grain boundary of two adjacent β-Si_3N_4 grains (spots 4 and 5, Fig. 4). Carbon introduced with the crystalline starting α-Si_3N_4 powder is supposed to be distributed at the grain boundaries after phase transformation and grain growth. No significant change in C concentration at the sub-grain boundary was observed. This impurity, detected by neutron activation analysis in the original β-Si_3N_4 whiskers (see Table 2) was probably rejected from the whisker surface during the phase transformation and grain growth step. Carbon collected at the microstructural grain boundaries as shown in Fig. 4, spots 4 and 5.

The difference between the two triple-points C and D, respectively, is mainly in the ratio of Si to the other elements (Al, Y, O, N). This ratio is much higher for triple-point C. The ratio of Al/Y is almost the same for both triple-points, C and D. The ratio N/Y is much higher for triple point C and the ratio O/Y is higher for triple point D, as is seen from Fig. 5 (EDX analysis of both triple points). These differences reflect the local chemistry of the triple points. Further analysis of other triple points was performed. This can be summarized as follows. The triple points can be divided into two principal types, amorphous and crystalline even within the samples crystallized according to the procedure described above. The amorphous triple points have in all analyzed cases almost the same EDX pattern as for the triple point D. The solubility of elements present in the starting powder in this glass is quite high, although one exception seems to be nitrogen. Two types of crystallized triple points were investigated. The first type, the triple points intrinsic to the microstructure as a result of annealing (an example is the triple point C, Fig. 3) and the second type, the triple points crystallized from amorphous triple points *in situ* by the electron beam.

The TEM of amorphous triple points crystallized *in situ* (Fig. 6) contained several types of crystalline phases. The EDX pattern of the first phase [Fig. 7(a)], only Si, Y and O revealed (presence of carbon must be neglected because of carbon coating for this set of measurements). The same pattern was obtained also for triple points found after annealing in the furnace as described above. This finding corresponds with the X-ray measurements on the cut surfaces of annealed bulk samples in which, as minor crystallized phases $Y_2Si_2O_7$ and/or Y_2SiO_5 were identified. The other EDX pattern obtained from the other spot of the same in-situ crystallized triple point is shown in Fig. 7(b). The

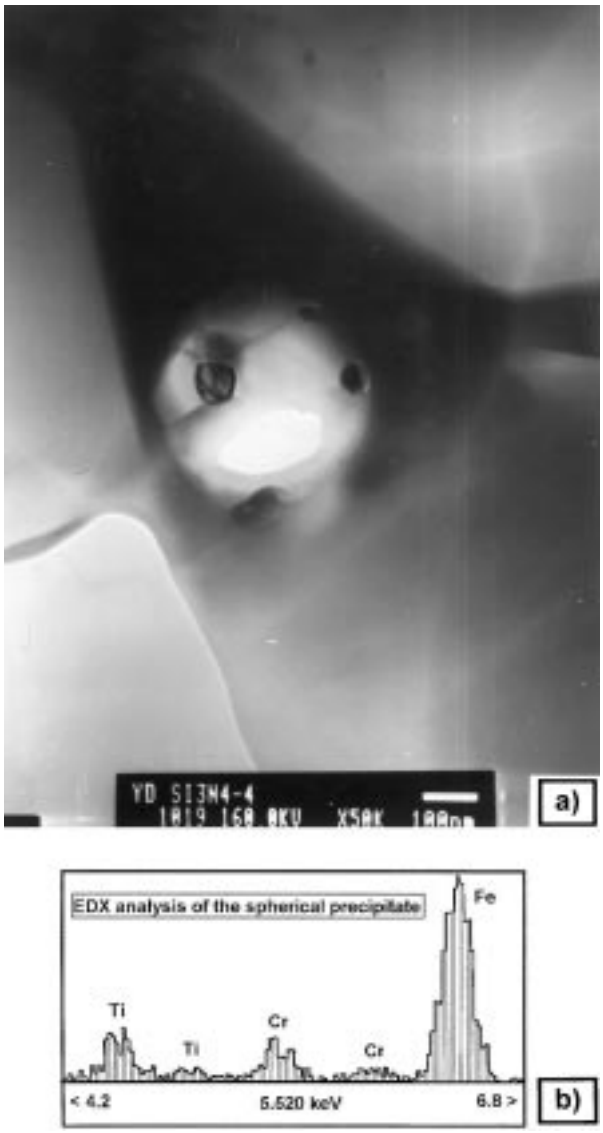

Fig. 8. (a) TEM micrograph of spherical object found in the triple point after in-situ crystallization; (b) its EDX pattern.

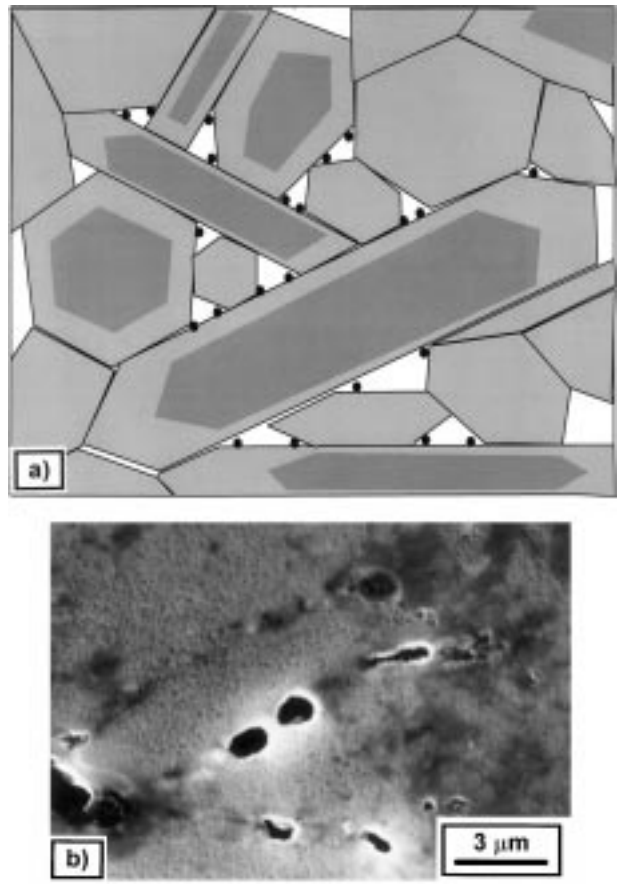

Fig. 9. (a) Schematic of possible distribution of segregated impurities (black spots) after crystallization of triple-points; (b) cavity formation at the whisker–matrix interface.

ratio of Si to minor elements Y, N, O is much higher compared to previous crystalline phase and the presence of Al and N is confirmed. This pattern is very similar to those obtained for triple point C, Fig. 4. These analyses reveal the different local chemistry of nano-grains crystallized from the liquid within the same sample, even within the same triple point. The crystallized phases in all cases consist of the main elements introduced along with the starting powders, i.e. Si, N, Al, Y and O. The starting powder impurities were not found in these crystallized phases. On the other hand, a second phase in size range of 50 to 500 nm was identified within the crystallized triple-points, Fig. 6, as indicated by the arrow. Higher magnification of this object is shown in Fig. 8(a) and the EDX analysis is shown in Fig. 8(b). This reveals very high concentration of Fe. Presence of Cr, Ti and Cu was also confirmed. The majority of these elements were analyzed as impurities in the starting β-Si_3N_4 whiskers. While these impurities were probably uniformly dissolved in the glassy pockets (triple points) with concentrations below the detection limit of EDX after crystallization, the particular phases could be identified.

The schematic of their possible distribution is shown in Fig. 9(a). This experimental result helps to understand the high temperature behavior of this kind of composite. Figure 9(b) shows cavity formation on the whisker–matrix interface of the composite prepared within this study after a four-point bending test at 1200°C. The impurity-enhanced intergranular cavity formation during the creep test is in agreement with the observations of Tanaka *et al.*[8] The difference is that their 'impurity enhanced cavity formation' model is based on the atomic diffusivity in the presence of the impurities at elevated temperature and local stress; the present observation suggests concentration of the impurities following crystallization of the major additives at the triple points and consequent local decrease of the eutectic temperature. The locally melted spots along with carbon present at grain boundaries, (Fig. 4) are probably responsible for the cavities of size several hundred nm observed and shown in Fig. 9(b).

4 Conclusions

The temperature of liquid phase formation some 150°C lower than the temperature from the phase diagram is a consequence of the impurities introduced along with the starting powders. These impurities are dissolved in the liquid phase and after cooling are present in the glassy triple pockets of the microstructure. Their concentration is under the EDX detection limit.

After annealing of samples at high temperature (1200–1440°C), the triple pockets within the same sample are either in the crystalline or amorphous state. The crystalline phases identified within the crystallised triple points are $Y_2Si_2O_7$ and Y_2SiO_5. Within these crystalline triple points the segregation of impurities was observed. Segregated impurities represent regions with higher concentration of Fe. The Cr, and Ti are also present in lower amounts, as detected by EDX.

The distribution of these concentrated impurities within the triple points is considered a reason for cavity formation during creep tests of the crystallized samples, owing to the local reduction in the eutectic temperature.

Acknowledgements

The authors acknowledge the support of US–Slovak Science and Technology Program, project no. 94039 and partial support Slovak Grant Agency VEGA, project 2/5118/98.

References

1. Heinrich, J. G., Krütner, H., Silicon nitride materials for engine applications. In *Tailoring of Mechanical Properties of Si_3N_4 Ceramics*, ed. M. J. Hoffmann and G. Petzow. NATO ASI Seies E: Applied Sciences, Vol. 276, Kluwer Academic Publisher, Dordrecht, 1994, pp. 415–427.
2. Matsui, M., Masuda, M., Fracture behavior of silicon nitride at elevated temperatures. In *Tailoring of Mechanical Properties of Si_3N_4 Ceramics*, ed. M. J. Hoffmann and G. Petzow. NATO ASI Seies E: Applied Sciences, Vol. 276, Kluwer Academic Publisher, Dordrecht, 1994, pp. 403–414.
3. Martins, C. S., Steen, M., Bressers, J., Rosa, L. G., Mechanical performance of commercial silicon nitride pre-exposed to sulphidizing atmosphere at high temperature. In *Tailoring of Mechanical Properties of Si_3N_4 Ceramics*, ed. M. J. Hoffmann and G. Petzow. NATO ASI Seies E: Applied Sciences, Vol. 276, Kluwer Academic Publisher, Dordrecht, 1994, pp. 415–427.
4. Mörgenthaler, K. D., Bühl, H., Ceramics for engines. In *Tailoring of Mechanical Properties of Si_3N_4 Ceramics*, ed. M. J. Hoffmann and G. Petzow. NATO ASI Seies E: Applied Sciences, Vol. 276, Kluwer Academic Publisher, Dordrecht, 1994, pp. 429–441.
5. Lewis, M. H., Crystallisation of grain boundary phases in silicon nitride and SiAlON ceramics. In *Tailoring of Mechanical Properties of Si_3N_4 Ceramics*, ed. M. J. Hoffmann and G. Petzow. NATO ASI Seies E: Applied Sciences, Vol. 276, Kluwer Academic Publisher, Dordrecht, 1994, pp. 217–231.
6. Granger, G. B., Crampon, J. and Duclos, R., Glassy grain-boundary phase crystallisation of silicon nitride: kinetics and phase development. *J. Mater. Sci. Lett.*, 1995, **14**, 1362–1365.
7. Bodur, C. T., Effects of heat treatments on the creep properties of a hot-pressed silicon nitride ceramics. *J. Mater. Sci. Lett.*, 1995, **30**, 1511–1515.
8. Tanaka, I., Pezzotti, G., Matsushita, K., Miyamoto, Y. and Okamoto, T., Impurity-enhanced intergranural cavity formation in silicon nitride at high temperatures. *J. Am. Ceram. Soc.*, 1991, **74**(4), 752–759.
9. Šajgalík, P. and Dusza, J., Reinforcement of silicon nitride by β-Si_3N_4 whiskers. *J. Euro. Ceram. Soc.*, 1989, **5**, 321–326.
10. Šajgalík, P. and Dusza, J. Development of β-Si_3N_4 reinforced Si_3N_4 ceramics. In *EURO-CERAMICS II, Vol. 2: Structural Ceramics and Composites*, ed. G. Ziegler and H. Hausner. D. K. G., Cologne, 1992, pp. 1589–1593.
11. Dusza, J., Šajgalík, P., Bástl, Z., Kavečanský, V. and Durišin, J., Properties of β-silicon nitride whiskers. *J. Mater. Sci. Lett.*, 1992, **11**, 208–211.
12. Murakami, Y. and Ymamoto, H., Phase equilibria in Al_2O_3–Y_2O_3–SiO_2 system and phase separation and crystallisation behavior of glass. *J. Ceram. Soc. Jpn.*, 1991, **99**(3), 215–221.
13. Šajgalík, P. and Galusek, D., α/β phase transformation of silicon nitride: homogeneous and heterogeneous nucleation. *J. Mater. Sci. Lett.*, 1993, **12**, 1937–1939.
14. Krämer, M., Hoffmann, M. J. and Petzow, G., Grain growth studies of silicon nitride in an oxynitride glass. *J. Am. Ceram. Soc.*, 1993, **76**(111), 2778–2784.